International Journal for Computational Civil and Structural Engineering, 18(3) 25–36 (2022)

DOI:10.22337/2587-9618-2022-18-3-25-36

ON THE CALCULATIONS FOR THE STABILITY OF BEAMS, FRAMES, AND CYLINDRICAL SHELLS IN THE ELASTO-PLASTIC STAGE

Gaik A. Manuylov, Sergey B. Kosytsyn, Maxim M. Begichev

Russian University of Transport, Moscow, RUSSIA

Abstract. The problems of stability of some beams, П-shaped frames and cylindrical shells with the elasto-plastic material are considered. The possibility of modeling bars using finite elements of various types is studied. Plate elements and even one-dimensional beam finite elements can be used for modelling compressed rods with geometric and physical nonlinearity. For the problem of stability of a circular cylindrical shell is given the comparison of the authors' results obtained using the FEM with the experimental results of V.G. Sazonov and the calculations of A.V. Karmishin.

Keywords: stability, geometric nonlinearity, physical nonlinearity, finite element method

О РАСЧЕТАХ НА УСТОЙЧИВОСТЬ СТЕРЖНЕЙ, РАМ И ЦИЛИНДРИЧЕСКИХ ОБОЛОЧЕК В УПРУГО ПЛАСТИЧЕСКОЙ СТАДИИ

Г.А. Мануйлов, С.Б. Косицын, М.М. Бегичев

Российский университет транспорта, Москва, РОССИЯ

Аннотация. В работе рассматриваются вопросы устойчивости некоторых стержней, П-образных рам и цилиндрических оболочек в упруго пластической стадии работы материала. Рассмотрена возможность моделирования стержней при помощи конечных элементов различных типов. Показано, что для расчета сжатых стержней с учетом геометрической и физической нелинейности можно использовать плоские и даже одномерные конечные элементы. Для задачи устойчивости круговой цилиндрической оболочки приведено сравнение результатов авторов, полученных при помощи МКЭ с результатами экспериментов В.Г. Сазонова и расчетами А.В. Кармишина.

Ключевые слова: устойчивость, геометрическая нелинейность, физическая нелинейность, метод конечных элементов

1. ANALYSIS OF DIFFERENT TYPES OF FINITE ELEMENTS IN THE STABILITY PROBLEMS WITH GEOMETRIC AND PHYSICAL NONLINEARITIES

Let us investigate the possibilities of various finite element models concerning the geometrically and physically nonlinear problem of stability of a cantilever beam. The beam had a length l=100 cm and a square cross section 10×10 cm, beam flexibility

$$\lambda = Ml/\sqrt{EJ} = 69.$$

This value is less than the limiting flexibility for a beam with such geometrical parameters made of steel 10HSND ($\lambda_* = 72$). The study used the model of an ideal Prandtl elasto-plastic material (σ_{yeiled}=400 MPa). Four types of finite element models are considered:

1. Using solid finite elements (FE) in the NASTRAN complex (Hex8);
2. Using plate FE with loss of stability in the element plane;

3. Using plate FE with loss of stability out of the element plane;

4. Using beam FE.

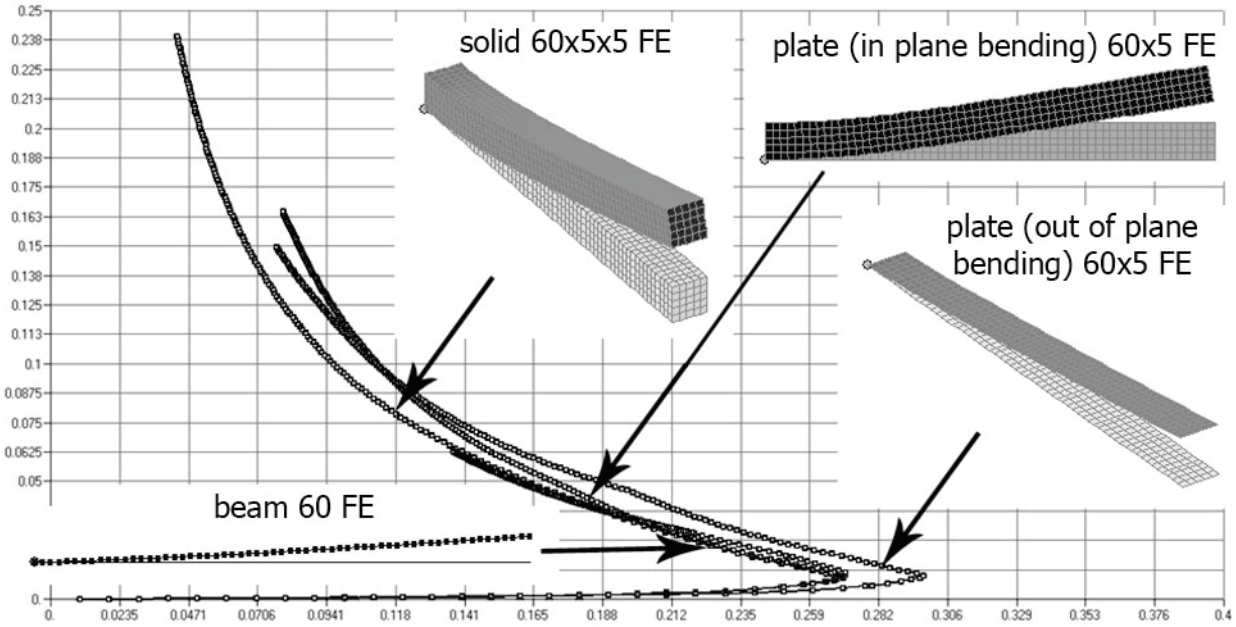

Figure 1. Curves of deformation development of an axially compressed cantilever beam

It was found that when using a three-dimensional model (5x5x60 cubic elements) of the above-described axially compressed beam, a model of 60 one-dimensional beam elements, as well as flat square four-node FE (5 plate elements along the height of the section, located in the plane of loss of stability), the critical loss of stability loads at limiting points and post-critical curves of unstable equilibrium states, almost coincided (Fig. 1).

A slightly higher compression load ($\Delta P_{cr} \approx 9\%$) had the model of a plate elements, bending at loss of stability "out of its plane". It follows from this that to solve physically and geometrically nonlinear stability problems it is not necessary to use models of beams from three-dimensional finite elements. Two-dimensional plate elements (and even one-dimensional beam elements) make it possible to obtain acceptable results in majority of loss of stability problems taking with elasto-plastic material behavior. The use of such elements significantly reduces the dimension of stability problems (in comparison with solid FE), and, as a consequence, reduces the time for their solution.

2. ECCENTRICALLY COMPRESSED CANTILEVER BEAM

In this paragraph, on the model (1200 flat four-node FE) of the cantilever beam (lenght l = 1,2 m) which has a nonlinear material diagram with hardening (Fig. 2, $\sigma = \varepsilon E - -k\varepsilon^3/3, E = 2{,}1 \cdot 10^6\ kg/cm^2$) and unloading according to a linear law, the influence of the initial imperfections in the application of a compressive force (offset) to the end section by the value of the loss of stability critical load.

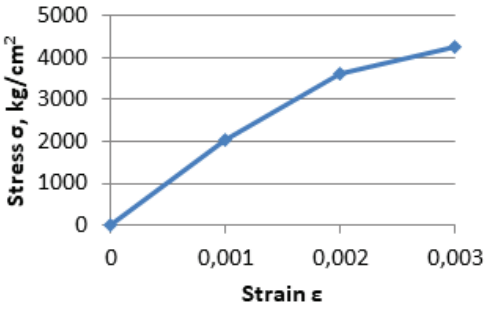

Figure 2. Stress-strain diagram for the material of the cantilever beam

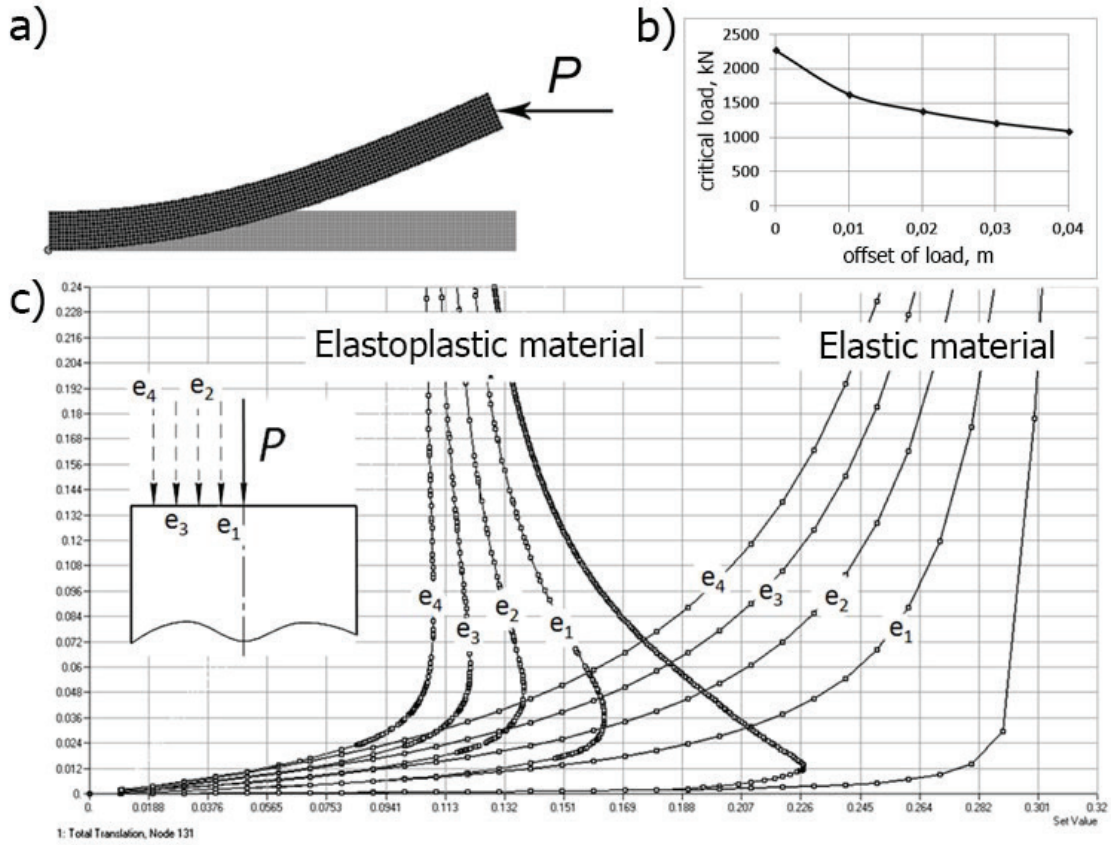

Figure 3. Elasto-plastic buckling of a cantilever axially compressed beam: a) deformed form of the beam; b) a graph of reduction of the values of critical loads; c) curves of displacement of the end of the beam

Imperfections in this problem were set in the form of different values of the offset of the point of the force application with respect to the center line of the beam (Fig. 3). A series of curves of equilibrium states was obtained for a beam made of an linear elastic material and for an elastoplastic rod made of a material with the above mentioned deformation law (Fig. 2). For a beam with a linear elastic material model, the curves of equilibrium states increase smoothly with increasing load, since the loss of stability of a linear elastic axially compressed beam occurs at the point of symmetric stable bifurcation [1,2].

When the material of the beam obeys the diagram of elasto-plastic deformation, the bifurcation point becomes unstable (in the formulation of the Euler-Karman problem), and the cantilever axially compressed beam loses its stability «in large» (Fig. 3a). In this case, the drop in the critical loads values turns out to be strongly dependent on the magnitude of the initial imperfections (indicated offsets) (Fig. 3c). The graph of the dependence of the critical loads at the limiting points on the offset value shown in Fig. 3b demonstrates that when the load was displaced from the axis by 0.01 m (the minimum used offset value) its critical value decreased by ~ 30%, and at a maximum offset of 0.04 m by ~ 52%. This confirms the well-known statement of T. Karman about the extremely high sensitivity of short beams (beams that lose their stability in the elasto-plastic stage of material operation) to the initial application of compressive load' offsets [3].

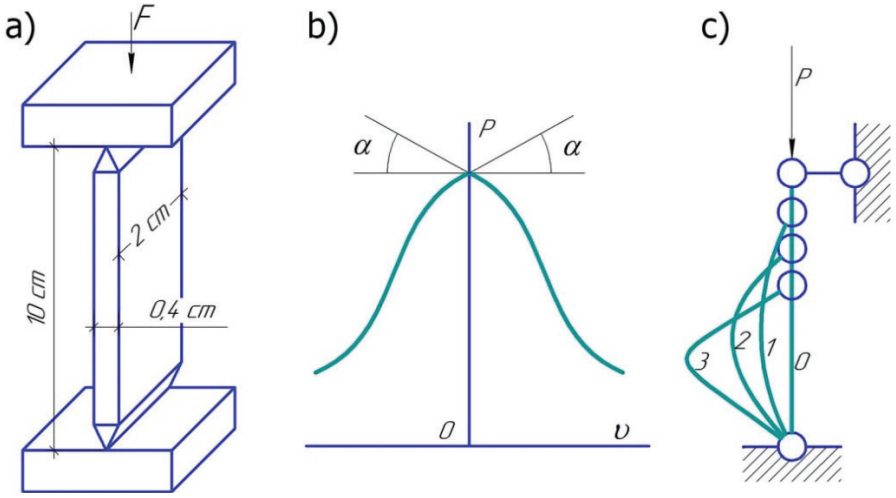

Figure 4. Compressed pivotally supported beam

3. ON THE LOSS OF STABILITY OF A COMPRESSED PIVOTALLY SUPPORTED BEAM IN THE ELASTO-PLASTIC STAGE

A flat steel beam 10×2×0.4 cm (St. 3) is used to qualitatively demonstrate the loss of stability effects in the elastoplastic stage under kinematic loading in a press (Fig. 4a). Beam characteristics $A = 0{,}8\ cm^2$, $J_{min} = 1{,}07\ cm^4$, $\lambda = 86{,}6 < 100$.

The beam had hinged boundary conditions. According to the Tetmayer's formula:

$$\sigma_{crit} = 3100 - 11{,}4, = 2112{,}7\ kg/cm^2,$$
$$P_{crit} = \sigma_{crit}\, A = 1690{,}2\ kg$$

The actual critical load observed during experiment is less than 1690 kg. This is explained by the high sensitivity of the critical load to the initial offsets of load, since here the curve of the initial post-critical equilibrium is unstable (with a bend at the apex at P = P_{crit}, Fig. 4b).

The moment of loss of stability of the elasto-plastic beam onset corresponds to the maximum load. At the beginning of buckling, the beam is slightly bent along a curve close to a sinusoid. But unlike elastic loss of stability, the "new" compressed-bent equilibrium is unstable. The beam, as it were, "slips out" of the decreasing pressure in the press. At the same time, its shape is changing. The curvature of the middle zone of the beam becomes larger and larger. On the contrary, the zones adjacent to the supports try to "straighten out". In the end, the rod takes the shape of an angle of $\sim 130° - 140°$ with a concentration of curvature near the middle section (Fig. 4c). In fact, a plastic hinge is formed here.

The calculation of such a beam was carried out with the NASTRAN (2520 FE plate) to construct the equilibrium diagrams shown in Fig. 5. The calculated diagram σ – ε was taken as Prandtls diagram with a yield point $\sigma_{yield} = 2400$ kg/cm^2. The critical load was 1800 kg. But this is not the result of loading in the form of pure compression. The beam bending was provoked by a "small" lateral force Q = 30 kg. When performing a geometrically nonlinear calculation, such a "disturbing" force is required. But this force causes imperfections, to which the "elasto-plastic" beam is very sensitive.

Fig. 5 shows the sequential development of stresses and deformations in the middle zone of the test sample after loss of stability in the elasto-plastic stage of material operation. The beginning of the formation of the plastic hinge - points 1 and 2. But if point 1 corresponds to the maximum load, then in point 2 the load dropped to $\sim 0{,}3\ P_{max}$. In points 3 and 4, the compressive load is even smaller. However, the zone of

compressive stresses (blue) has increased (along the depth of the section). Finally, for point 5, the plastic hinge extended about ¼ along the length of the sample.

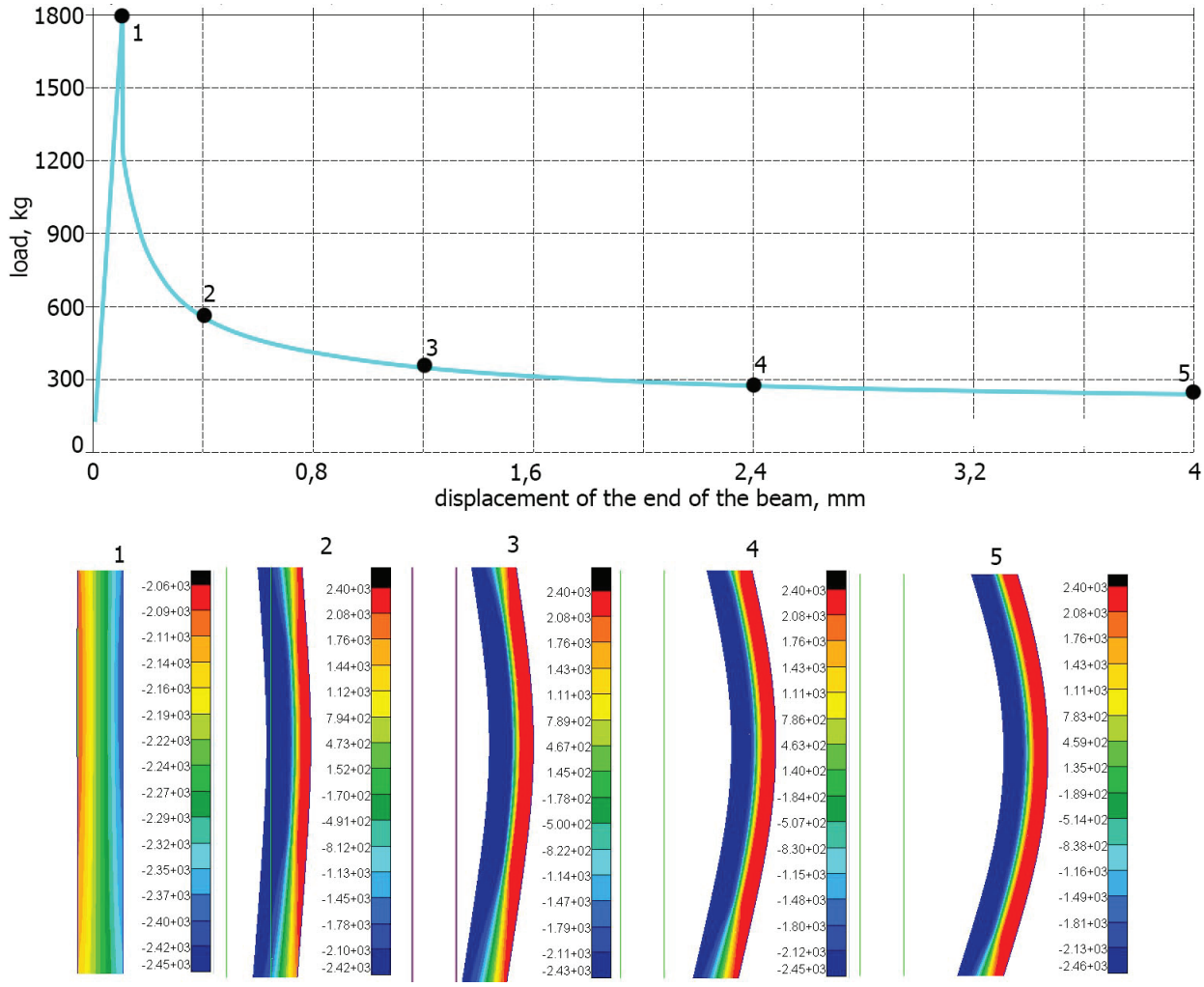

Figure 5. The equilibrium diagram for the compressed pivotally supported beam

4. ON SOLUTIONS OF ELASTO-PLASTIC PROBLEMS OF STABILITY OF FRAMES

It is known that the solution of elastoplastic problems can be determined using two different approaches: the theory of small elastoplastic deformations and using the flow theory. According to the first theory, the relationship between stresses and deformations turns out to be finite; according to the flow theory, these relations are differential.

If the loading is simple, then both theories of plasticity give the same results.

If the loading is not simple, then the results obtained using the flow theory, usually, match better the experimental data in comparison with the results given by the theory of small elasto-plastic deformations.

Solutions for both theories are obtained as a result of the convergence of iterative processes. The FE-complex NASTRAN implements the solving procedure according to the flow theory. In the semi-automatic version of the stability problems for frame systems in the elasto-plastic stage solution, it is convenient to use the theory of small elasto-plastic deformations with

iterations by the method of elastic solutions with variable elastic parameters.
The convergence of this iterative process in the general case has not been rigorously proven. However, numerous calculations show that for ordinary "convex" (broken or smooth) $\sigma - \varepsilon$ diagrams, the iterations converge to such a solution.

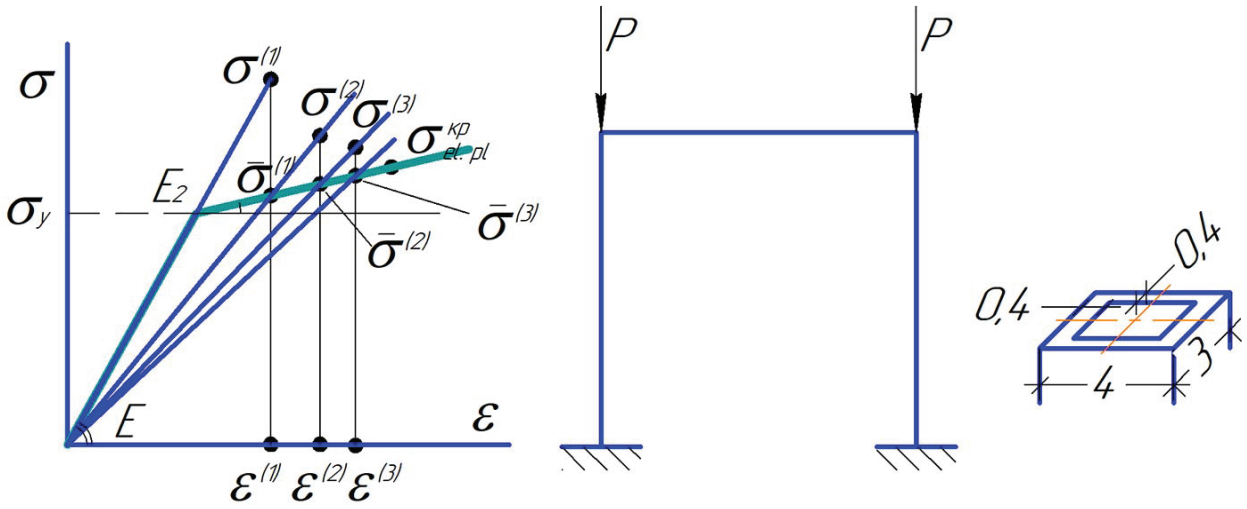

Figure 6. The variable parameters of elasticity method.

The essence of the variable parameters of elasticity in stability problems method will be explained using Fig. 6.
Let the material have a bilinear $\sigma - \varepsilon$ diagram with modules E and E_2. The first approximation is the result of solving the elastic stability problem. If the critical "elastic" stresses of the first approximation

$$\sigma^{(1)} = \frac{P_{cr\ elast}}{A} = \frac{P^{(1)}}{A}$$

is greater than the yield stress $\sigma_{yieled}\left(\sigma^{(1)} > \sigma_{yieled}\right)$this means that the frame loses its stability in the elastoplastic stage. The stress $\sigma^{(1)}$ is the first upper approximation for $\sigma^{cr}_{elast-pl}$. Next, we find the relative deformation

$$\varepsilon^{(1)} = \frac{\sigma^{(1)}}{E},$$

and stress $\bar{\sigma}^{(1)}$ in the second section of the $\sigma - \varepsilon$ diagram

$$\bar{\sigma}^{(1)} = \sigma_{yieled} + (\varepsilon^{(1)} - \varepsilon_{yieled})E_2$$

Here $E_2$is the slope modulus in the second section. The stress $\bar{\sigma}^{(1)}$ gives lower bound $\sigma^{cr}_{elast-pl}$. As a result, we have the first two-sided estimates

$$\bar{\sigma}^{(1)} < \sigma^{cr}_{elast-pl} < \sigma^{(1)}$$

Next, a new elasticity modulus is calculated $E^{(2)}$

$$E^{(2)} = \frac{\bar{\sigma}^{(1)}}{\varepsilon^{(1)}} < E^{(1)}$$

This module takes into account the decrease in the bending stiffness of the compressed beams at the second iteration compared to the original module E. The reduction factor

$$\Psi^{(1)} = \frac{E^{(2)}}{E} < 1$$

is a multiplier as well in the bending stiffness of compressed beams,

$$\frac{EJ}{l} \to \frac{\Psi EJ}{l},$$

as in the new force parameter $\nu^{(2)}$

$$\nu^{(2)} = l\sqrt{\frac{N}{\Psi ET}} = \frac{\nu}{\sqrt{\Psi}^{(2)}}$$

The solution of the characteristic equation of the second approximation gives the critical parameter $\nu_{cr}^{(2)}$ and the critical force $P^{(2)}$

$$P^{(2)} = \left(\nu_{cr}^{(2)}\right)^2 \Psi^{(2)} \frac{ET}{l^2}$$

Then all calculations of $\sigma^{(2)}, \varepsilon^{(2)}$and $\bar{\sigma}^{(2)}$ are repeated. As a result, we obtain new improved two-sided estimates ($\sigma^{(2)} < \sigma^{(1)}, \bar{\sigma}^{(2)} > \bar{\sigma}^{(1)}$).

$$\bar{\sigma}^{(2)} < \sigma_{elast-pl}^{cr} < \sigma^{(2)}$$

Iterations continue until the first few digits match in the values $\sigma^{(n)}$and $\sigma^{(-n)}$. Usually, two or three correct signs are enough for $\sigma_{elast-pl}^{cr}$.

As an example, let us consider the solution of the elasto-plastic stability of a U-shaped frame with a box-shaped cross-section of 3×4 cm and 0.4 cm thick walls by the method of variable elastic parameters problem. Here: $l = 100$ cm, $A = 4{,}96$ cm^2, $J = 10\ cm^4$, $E_1 = 2 \cdot 10^6\ kg/cm^2$, $E_2 = 0{,}6 \cdot 10^6\ kg/cm^2$. The stress $\sigma_{yieled} = 2000$ кг/см^2 (bilinear diagram).

The characteristic equation of the first approximation (elastic problem) and its solution is

$$6\frac{EJ}{l} + \frac{EJ}{l} * \frac{\nu}{tg\ \nu} = 0,\ \ \nu^{(1)} = 2{,}716,$$

$$\nu = l\sqrt{\frac{P}{EJ}}.$$

$$P^{(1)} = \frac{2{,}716^2 * 2 * 10^6 * 10}{10^4} = 14753{,}3\ kg,$$

$$\sigma^{(1)} = \frac{P^{(1)}}{A} = 2974{,}4\ kg/cm^2$$

$$\varepsilon^{(1)} = \frac{\sigma^{(1)}}{E_1} = 1{,}48723_{-3},\ \ \varepsilon_{prop} = 10^{-3},$$

$$\bar{\sigma}^{(1)} = 2000 + (1{,}48723_{-3} - 1_{-3})0{,}6 * 10^6 = 2292{,}3\ kg/cm^2$$

Thus, after the first iteration step, we have the estimates

$$\left(2292{,}3 < \sigma_{elast-pl}^{cr} < 2974{,}4\right) kg/cm^2$$

The new elasticity modulus for the second iteration

$$E^{(2)} = \frac{\bar{\sigma}^{(1)}}{\varepsilon^{(1)}} = \frac{2294{,}3}{1{,}48723_{-3}} \cong 1541347\ \frac{\text{кг}}{\text{см}^2},$$

$$\Psi^{(2)} = \frac{E^{(2)}}{E} = 0{,}77$$

Characteristic equation of the second iteration

$$6\frac{EJ}{l} + 0{,}77\frac{EJ}{l} * \frac{\nu_2}{tg\ \nu_2} = 0,\ \ \nu_{2\ cr} \cong 2{,}8, \nu_{cr}^{(2)} = \frac{\nu_{2\ cr}}{1{,}139} = 2{,}458$$

Continuing the calculations, we obtain the estimates

$$\left(2348{,}4 < \sigma_{elast-pl}^{cr} < 2436\right) kg/cm^2$$

The third iteration gives

$$\left(2353 < \sigma_{elast-pl}^{cr} < 2360\right) kg/cm^2$$

We restrict ourselves to the third approximation and assume that $\sigma_{elast-pl}^{cr} \cong 2356\ kg/cm^2$. Critical load $P_{cr.\ elast-pl} = 11688{,}6$ kg.

It is interesting to note that according to the solution using a beam FE at $\varepsilon = 1/100000$, the

critical load turned out to be very close to the calculated one ($P^{cr}_{elast-pl}\ (beam) = 11739\ kg$). However, when comparing with the results ($P^{cr}_{elast-pl}$~9880,5 kg) obtained with the help of plate FE, one can see the difference (~16.5%) in the critical force. There are no convincing explanations for this discrepancy yet. It is impossible to explain the difference between the flow theory and the theory of small elasto-plastic deformations, since the result $P^{cr}_{elast-pl}$, obtained using the beam FE was calculated according to the theory of flows ($P^{cr}_{elast-pl} = 11739\ kg$), and, as shown above, is in good agreement with the value of $P^{\text{ск}}_{elast-pl}$ obtained on the basis of the theory of small elasto-plastic deformations ($P^{cr}_{elast-pl} = 11688\ kg$). Let us consider additional solutions to the problem of elasto-plastic buckling of a U-shaped frame (Fig. 7), composed of 100 cm long beams and having 4 × 3 cm rectangular tubular sections 0.4 cm thick. The analytic model of the frame is made up of 10492 plate FE (NASTRAN). The lower sections of the frame struts are sealed. Nodal load (two vertical compressive forces P). The diagram of material operation is bilinear with module $E = 2 \cdot 10^6\ kg/cm^2$ in the first section and module $E_2 = 0{,}3\ E = 0{,}6 \cdot 10^6\ kg/cm^2$ for the second section ($\sigma_T = 2000\ kg/cm^2$). The imperfections were specified in the form of 2 small horizontal nodal forces εP, where ε = 0.0000022; 0.00001; 0.0001; 0.001 and 0.01. With such imperfections, the critical loads are 98.805; 98.7; 97.65; 90.36 and 71.04 (kN). As can be seen from the above results, with the loss of stability in the elasto-plastic stage, the drop in the critical load with an increase in the "forced" initial imperfections is quite noticeable. This is a significant difference from the "elastic" loss of stability (stable symmetric bifurcation), the curves of the initial supercritical equilibrium at ε = 0 and ε = 0.001 are very close to each other (Fig. 7).

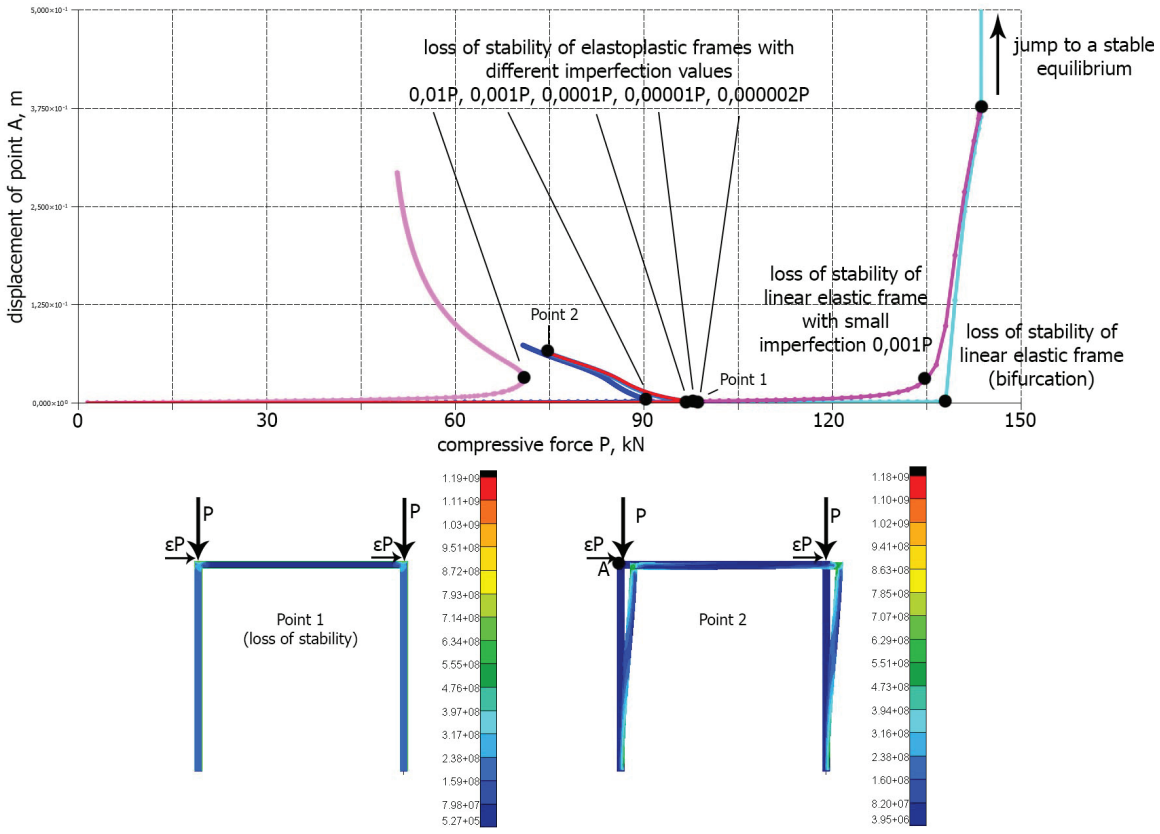

Figure 7. Deformation diagrams of U-shaped frame with different initial imperfections

The sensitivity of the elasto-plastic critical load to initial imperfections exists due to the fact that the post-critical equilibrium of the frame after elasto-plastic loss of stability is unstable.

The nature of a sharp decrease in elasto-plastic critical loads is clearly visible in Fig. 7. At ε = 0.01 ΔPcr% = (98.8−71.04)/98, 8·100% ≅ 28%. That is quite a lot.

Note that when using plate elements and a nonlinear elastic material model, the critical loads (98.2 kN at ε = 0.00001 and 98.65 kN at $\varepsilon = \frac{1}{500000}$) practically coincided with the corresponding values from the elastic-plastic calculation.

An attempt was made to use a beam FE element. For a linearly elastic material, the results of calculating $P_{\text{кр}}$ turned out to be quite close to those calculated "manually".

$$P_{cr\ elast} = 147{,}54\ kN\ =>$$
$$2{,}716^2 \cdot 2 \cdot 10^6 \cdot \frac{10}{10^4}\ kg = 147533\ kg$$

However, the elasto-plastic calculation gave a significantly lower critical force ($P_{cr\ elast-pl} \cong 117{,}4\ kN$). The obtained value of the critical load on the NASTRAN is in good agreement with the result of the calculation by the method of variable parameters of elasticity (~ 117 kN).

5. STABILITY OF A CIRCULAR CYLINDRICAL SHELL UNDER AXIAL COMPRESSION

Let us compare the study results on the stability of a circular cylindrical shell under axial compression made by the author (numerical simulation according to the NASTRAN FEM) with the results of experiments by V.G. Sazonov and the calculations of A.V. Karmishin, given in the book [4].

Three series (each with six samples) of shells with length L = 136 mm, outer diameter d = 79 mm and thicknesses h = 1.0; 1.5; 2.0 mm were subjected to tests. The shells were made from pipes and checked for wall thickness differences (± 2%). The shell material - AMG6. The material diagram is shown in Fig. 8, the values of ε and σ are given in Table 1.

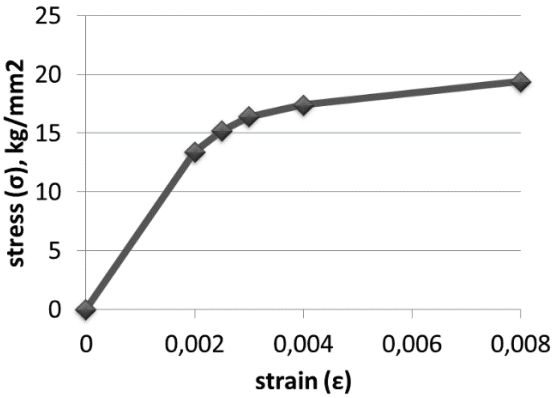

Figure 8. Stress-strain diagram of the elastoplastic material AMG6

Table 1. Coordinates of the AMG6 stress-strain diagram

Point №	strain	stress, kg/mm^2
1	0	0
2	0,002	13,40
3	0,0025	15,20
4	0,003	16,40
5	0,004	17,40
6	0,008	19,40

Tests of shells with h = 1 mm and h = 1.5 mm were carried out on a laboratory machine with a mechanical wire ZDM-10, shells with h = 2 mm - on a machine with a Sapper-100 hydraulic drive. The alignment of the models was ensured by marking the machine plates. To prevent distortions, ball joints were used (this is evidenced by stable test results). The models loading was carried out in stages at a low speed. Fig. 8 shows the $\sigma_c(\varepsilon_c)$ diagrams obtained by recalculating the $P(\Delta)$ diagram using the formulas

$$\sigma_c = \frac{P}{2\pi Rh}, \qquad \varepsilon_c = \frac{\Delta}{L}.$$

At loads close to σ_A (Fig. 8), a pronounced bending deformation state is observed at the edges of the shell. The maximum deflection amplitude before the loss of stability reaches approximately 0.1 h.

When $\sigma = \sigma_A$ for shells with h = 1 mm and h = 1.5 mm, at one of the edges of the shell, the loss of stability occurs in an asymmetric shape, accompanied by a drop in stresses to $\sigma = \sigma_Б$, and the maximum deflection at the edge increases approximately up to 0.3h. However, the shell does not lose its bearing capacity, continuing to perceive the load. Then, at $\sigma = \sigma_Г$, the buckling shapes change and the shell loses its bearing capacity.

Shells with h = 2 mm also lose stability in their asymmetric shape, but no sharp drop in the load is observed. The buckling begins with the formation of four regular indentations along the ring, which increase with additional loading, and the load decreases.

When modeling cylinders by the finite element method, two material models were considered: an infinitely elastic and an elasto-plastic one based on the digitization of the diagram given in [4] (Fig. 8). The load was applied kinematically to the upper end of the shell through a rigid-element (absolutely rigid plate).

The obtained calculations results compared with the results of experiments by V.G. Sazonov and calculations by A.V. Karmishin are given in table 2.

The loss of stability in the experiment of V.G. Sazonov occurred at stresses corresponding to the flat section of the diagram.

Calculation using a nonlinear elastic model by A.V. Karmishin gave a good correlation with the experimental results (columns 2 and 3).

The curve of subcritical and supercritical equilibrium states for a shell 1 mm thick, obtained by NASTRAN, is shown in Fig. 10.

When using an elastic model of the material, the critical load on the shell was 22.8 kN (point 1 in Fig. 10, stress 93.2 kg / mm^2).

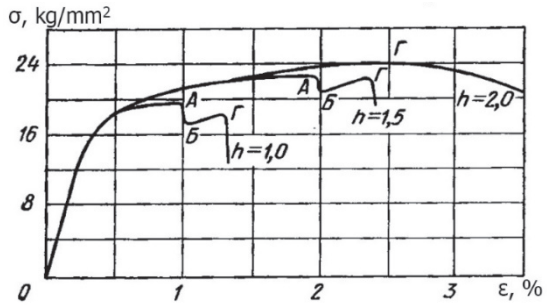

Figure 9. Experimentally obtained deformation diagrams of cylindrical shells

The subcritical equilibrium of the shell is axisymmetric; a nonlinear edge effect exists near the edges of the shell. Then the loss of stability occurs, and the shell goes into a distant stable equilibrium, characterized by the formation of a two-row belt of the rhombic-triangular indentations [5, 6] (Fig. 10 point 2). The compression load was reduced to 8.4 kN. With further loading, a secondary bifurcation occurs the restructuring of this belt into a three-row one (Fig. 10 point 3). After the loss of stability at point 2 (and under conditions of further loading), it turned out that the rigid element shifted and a skew appeared towards one part of the lateral surface of the shell. Cyclic symmetry has been lost.

The elasto-plastic equilibrium curve of the shell is completely different. Up to a load of $\sim 3{,}9\ kN$, the relationship between load and shortening is linear. Further, with a compression of $\sim 3{,}9\ kN$, a sharp increase in shortening was observed with a very weak increase in the load up to the limit point 4. (Fig. 10). Then the equilibrium of the shell became unstable. The development of dents was not along the entire lateral surface, but only near the end sections, in the zone of the elasto-plastic edge effect (point 5, Fig. 10).

Thus, it can be concluded that with the compressed circular cylindrical shells' elasto-plastic loss of stability, there is no "jump" in the load. However, it is 3.5-4 times less than the critical loads of elastic loss of stability.

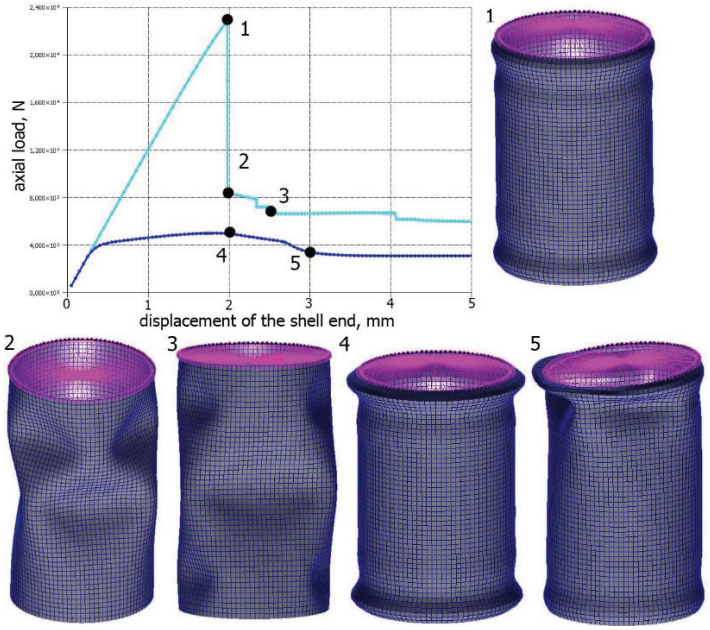

Figure 10. The diagram of the cylinder's deformation with a 1 mm thickness and a view of the model at characteristic points

Table 2. comparison of results of authors the results of experiments by V.G. Sazonov and calculations by A.V. Karmishin

Shell's thickness, mm	Critical stresses, kg/mm^2			
	Expiriment (V.G. Sazonov)	Plastic shell buckling (A.V. Karmishin)	Elastic analysis (Nastran)	Elasto-plastic analysis
1	2	3	4	5
1	19,5	19,2	93,20	20,45
1,5	22,6	21,4	148,11	25,75
2	23,9	22,6	178,84	30,55

REFERENCES

1. **Manuylov G.A., Kositsyn S.B., Begichev M.M.** Chislennoye modelirovaniye protsessov poteri ustoychivosti ravnovesiya tonkostennykh elementov konstruktsiy v usloviyakh uprugoplasticheskikh deformatsiy. Trudy Mezhdunarodnoy nauchno-prakticheskoy konferentsii «Inzhenernyye sistemy – 2011», Moscow, 05 – 08 april 2011. – Moscow: RUDN. – 2011. – p. 377-383.
2. **Manuylov G.A., Kositsyn S.B., Begichev M.M.** Sravnitel'nyy analiz ustoychivosti nekotorykh tonkostennykh konstruktsiy pri uprugikh i uprugo-plasticheskikh deformatsiyakh // Tezisy doklada 70 Nauchno-metodicheskoy i nauchno-issledovatelskoy konferentsii MADGTU (MADI). 30 january – 03 february 2012, Moscow: MADI, 2012 – p. 21 – 22.
3. **Timoshenko S.P.** Ustoychivost uprugikh sistem / M.: Ogiz, Gostekhizdat. – 1946. – 533 p.
4. **Karmishin A.V., Lyaskovets V.A., Myachenkov V.I., Frolov A.N.** Statika i dinamika tonkostennykh obolochechnykh

konstruktsiy. – Moscow: Mashinostroyeniye. – 1975. – 376 p.
5. **Manuylov G.A., Kositsyn S.B., Begichev M.M.** O yavlenii poteri ustoychivosti prodol'no szhatoy krugovoy tsilindricheskoy obolochki. chast 1: O poslekriticheskom ravnovesii obolochki // International Journal for Computational Civil and Structural Engineering Volume 12, Issue 3. – 2016. – p. 58-72.
6. **Manuylov G.A., Kositsyn S.B., Begichev M.M.** O yavlenii poteri ustoychivosti prodol'no szhatoy krugovoy tsilindricheskoy obolochki. chast II. Maksvellova sila i energeticheskiy bar'yer // International Journal for Computational Civil and Structural Engineering) Volume 12, Issue 4. – 2016. – p. 103-115.

СПИСОК ЛИТЕРАТУРЫ

1. **Мануйлов Г.А., Косицын С.Б., Бегичев М.М.** Численное моделирование процессов потери устойчивости равновесия тонкостенных элементов конструкций в условиях упругопластических деформаций // Труды Международной научно-практической конференции «Инженерные системы – 2011», Москва, 05 – 08 апреля 2011 г., М.: РУДН, 2011. С. 377 – 383.
2. **Мануйлов Г.А., Косицын С.Б., Бегичев М.М.** Сравнительный анализ устойчивости некоторых тонкостенных конструкций при упругих и упруго-пластических деформациях // Тезисы доклада 70 Научно-методической и научно-исследовательской конференции МАДГТУ (МАДИ). 30 января – 03 февраля 2012 г., М.: МАДИ, 2012 – С. 21 – 22.
3. **Тимошенко С.П.** Устойчивость упругих систем / М.: Огиз, Гостехиздат. 1946. - 533 с.
4. **Кармишин А.В., Лясковец В.А., Мяченков В.И., Фролов А.Н.** Статика и динамика тонкостенных оболочечных конструкций. – М.: Машиностроение. – 1975 г. – 376 с.
5. **Мануйлов Г.А., Косицын С.Б., Бегичев М.М.** О явлении потери устойчивости продольно сжатой круговой цилиндрической оболочки. часть 1: О послекритическом равновесии оболочки // International Journal for Computational Civil and Structural Engineering Volume 12, Issue 3. – 2016. – p. 58-72.
6. **Мануйлов Г.А., Косицын С.Б., Бегичев М.М.** О явлении потери устойчивости продольно сжатой круговой цилиндрической оболочки. часть II. Максвеллова сила и энергетический барьер // International Journal for Computational Civil and Structural Engineering) Volume 12, Issue 4. – 2016. – p. 103-115.

Gaik A. Manuylov, Ph.D., Associate Professor, Department of Structural Mechanics, Russian University of Transport; 127994, Russia, Moscow, 9b9 Obrazcova Street; phone/fax +7(499)972-49-81.

Sergey B. Kosytsyn, Dr.Sc., Professor, Head of Department of Theoretical Mechanics, Russian University of Transport; 127994, Russia, Moscow, 9b9 Obrazcova Street; phone/fax: +7(499) 978-16- 73; E-mail: kositsyn-s@yandex.ru, kositsyn-s@mail.ru

Maxim M. Begichev, Ph.D., Associate Professor, Department of Theoretical Mechanics, Russian University of Transport; 127994, Russia, Moscow, 9b9 Obrazcova Street; phone/fax: +7(499) 978-16-73; E-mail: noxonius@mail.ru.

Мануйлов Гайк Александрович, кандидат технических наук, доцент, доцент кафедры «Строительная механика» Российского университета транспорта; 127994, г. Москва, ул. Образцова, 9, стр. 9; тел./факс +7(499) 972-49-81

Косицын Сергей Борисович, доктор технических наук, профессор, заведующий кафедрой «Теоретическая механика» Российского университета транспорта; 127994, г. Москва, ул. Образцова, 9, стр. 9; тел./факс +7(499) 978-16-73; E-mail: kositsyn-s@yandex.ru, kositsyn-s@mail.ru

Бегичев Максим Михайлович, кандидат технических наук, доцент кафедры «Теоретическая механика» Российского университета транспорта; 127994, г. Москва, ул. Образцова, 9, стр. 9; тел./факс +7(499) 978-16-73; E-mail: noxonius@mail.ru.